

Sirt1 Regulates Corneal Epithelial Migration by Deacetylating Cortactin

Yong Lin,^{1,2} Qi Liu,^{1,2} Li Li,^{1,2} Rusen Yang,^{1,2} Juxiu Ye,^{1,2} Shuai Yang,^{1,2} Guangying Luo,^{1,2} Peter S. Reinach,^{1,2} and Dongsheng Yan^{1,2}

¹School of Ophthalmology and Optometry, Eye Hospital, Wenzhou Medical University, Wenzhou, Zhejiang, China

²State Key Laboratory of Ophthalmology, Optometry and Visual Science, Wenzhou, Zhejiang, China

Correspondence: Dongsheng Yan, School of Ophthalmology and Optometry, Eye Hospital, Wenzhou Medical University, Wenzhou, Zhejiang, China; dnaprotein@hotmail.com.

Received: May 4, 2022

Accepted: October 17, 2022

Published: November 9, 2022

Citation: Lin Y, Liu Q, Li L, et al. Sirt1 regulates corneal epithelial migration by deacetylating cortactin. *Invest Ophthalmol Vis Sci*. 2022;63(12):14.

<https://doi.org/10.1167/iovs.63.12.14>

PURPOSE. Silent information regulator 1 (SIRT1) is a nicotinamide adenine dinucleotide (NAD⁺) dependent deacetylase, which plays an essential role in cellular metabolism, autophagy, and chromatin accessibility. Our study aimed to determine its role in controlling corneal epithelial wound healing (CEWH).

METHODS. Corneal epithelial (CE)-specific *Sirt1* deletion mice were created using the Cre-lox system. CE debridement was used to create a CEWH model. Corneal epithelial cells (CECs) were collected with an Algerbrush. Western blot analysis and RT-qPCR were performed to determine protein and mRNA expression levels. siRNA transfection technology knocked down SIRT1 and cortactin expression levels in human corneal epithelial cells. Scratch wound assay, MTS assay, and TUNEL assay determined cell migratory, proliferative, and apoptotic behavior, respectively. Co-immunoprecipitation probed for SIRT1 and cortactin interaction. Immunofluorescence staining evaluated the location and expression levels of SIRT1, cortactin, acetylated-cortactin, and F-actin.

RESULTS. During CEWH, increases in SIRT1 mRNA and protein expression levels accompanied the downregulation of acetylated lysine in non-histone proteins. The loss of SIRT1 function reduced cell migration and, in turn, delayed CEWH. SIRT1 bound to and deacetylated cortactin in vitro and in vivo. Loss of either SIRT1 or cortactin suppressed wound edge lamellipodia formation, which is consistent with migration retardation.

CONCLUSIONS. During CEWH, SIRT1 upregulation and its modification of cortactin boost CEC migration by increasing the development of lamellipodia at the wound edge. Therefore SIRT1 may serve as a potential target to enhance CEWH.

Keywords: corneal epithelial wound healing, cortactin, migration, SIRT1

The integrity of the corneal epithelial layer is essential for maintaining corneal transparency and normal vision. Disruption of this outmost layer by injury or infection may lead to corneal opacification and degradation of optical acuity. If this occurs, resurfacing of areas where the barrier function has been weakened is required to restore normal corneal function. Numerous related growth factors,¹ cytokines,² and chemokines³ are involved in this renewal process by interacting with their cognate receptors and linked signaling pathways to mediate rises in gene and protein expression, which underpins cell proliferation and migration. It has been discovered recently that epigenetic modifications also play essential roles in corneal injury repair. Previously our group has found epigenetic modifications, including DNA methylation,⁴ histone methylation,⁵ and microRNAs,^{6,7} mediate corneal epithelial wound healing (CEWH). Histone modifications, such as acetylation and methylation occurring on histone H3 and H4, are common epigenetic markers of chromatin state.^{8,9} Such modifications have activating or inhibiting effects on the control of gene expression, regulating various biological processes. Here we aimed to explore the role of acetylation in regulating CEWH.

Lysine acetylation is one such post-translational modification that affects protein regulatory functions by changing its stability, activity, and interaction.¹⁰ Such changes affect a range of biological pathways, as well as stress responses and metabolism.¹¹ Changes in the acetylation status of proteins are a major form of epigenetic regulation in modulating cell proliferation and migration. However, there are few reports regarding this epigenetic modification involved in CEWH. Histone acetyltransferases and deacetylases (HDACs) are the enzymes that, respectively, add and remove acetyl groups from lysine residues on the histones and non-histone proteins.¹² SIRT1 is an NAD⁺-dependent class III HDAC that removes acetyl groups from histone and non-histone proteins. It regulates a wide variety of biological processes, including cell proliferation, migration, differentiation, and apoptosis, through deacetylating its substrates.¹³⁻¹⁶ Previous studies have shown that SIRT1 affects cell migration in a variety of malignancies,^{14,17,18} indicating that it is essential for controlling cell motility. Additionally, loss of SIRT1 is reported to inhibit angiogenesis and migration during skin wound repair.¹⁹ Regarding corneas, SIRT1 is richly distributed in the nucleus of corneal epithelial cells and

keratocytes.²⁰ Overexpression of SIRT1 promotes high glucose-attenuated corneal epithelial wound healing via p53 regulation of the IGFBP3/IGF-1R/AKT pathway.²¹ However, its specific role in mediating corneal epithelial responses underlying wound healing requires clarification.

We show here that SIRT1 is involved in regulating corneal epithelial renewal after injury. Furthermore, deleting this deacetylase selectively suppressed cell migration in corneal epithelial-specific *Sirt1* deletion mice. One of the reasons for the dependence of migration on SIRT1 expression is that it regulates the acetylation status of Cortactin that binds to actin filaments and contributes to mediating cytoskeletal regulation. Collectively, our findings underscore the significance of the SIRT1-Cortactin axis in regulating CEWH, suggesting SIRT1 might be a possibility for accelerating CEWH.

MATERIAL AND METHODS

Animals

Krt12-cre mice (B6.129 (Cg)-Krt12tm3 (cre) Wwk/J), which express CRE recombinase induced by the *Krt12* promoter,²² and *Sirt1^{lox/lox}* mice (B6; 129-*Sirt1*tm1Ygu/J), in which *loxP* flanked on both sides of exon4, were bought from The Jackson Laboratory (Bar Harbor, Maine, USA). *Krt12-Cre* mice were mated to *Sirt1^{lox/lox}* mice to generate heterozygous *Krt12-Cre⁺*, *Sirt1^{lox/+}* mice, which were then backcrossed to *Sirt1^{lox/lox}* mice to create *Krt12-Cre⁺*, *Sirt1^{lox/lox}* mice (*Sirt1* cKO). *Sirt1^{lox/lox}* mice or *Krt12-Cre⁺* mice were treated as the control counterparts. PCR examination of DNA extracted from tail biopsies verified the genotype of the mice. The PCR primer sequences were as follows: *Sirt1-flox* forward: 5'-GGT TGA CTT AGG TCT TGT CTG-3', *Sirt1-flox* reverse: 5'-CGT CCC TTG TAA TGT TTC CC-3'; *Krt12-wt* forward: 5'-CAG GAC TGA AAG CCC AGA CT-3', *Krt12-wt* reverse: 5'-AAG TCA CAG AGG CGG TAT GC-3'; *Krt12-cre* forward: 5'-CAG GAC TGA AAG CCC AGA CT-3', *Krt12-cre* reverse: 5'-CGG TTA TTC AAC TTG CAC CA-3'.

All the animal experiments were conducted in compliance with the recommendations of the Association for Research in Vision and Ophthalmology and approval of the Wenzhou Medical University Animal Care and Use Committee.

Corneal Epithelial Debridement

Corneal epithelial debridement was carried out as previously described.^{6,23} Briefly, eight-week-old C57BL/6 mice were anesthetized by intraperitoneal injection of ketamine (100 mg/kg body weight) combined with xylazine (10 mg/kg body weight), followed by topical application of proparacaine eye drops. A circular area of 2.0-mm diameter of cornea was labeled using a trephine blade, and the epithelial fragments were removed using an Alger brush II (The Alger Company, Inc, Lago Vista, TX, USA). The corneal epithelial layers were collected for RNA and protein analysis. The recovery of the epithelial wound was quantified by staining the debrided area with a drop of 1% sodium fluorescein and photographed using a slit-lamp bio-microscope with a Nikon D200 camera. Wounded areas were calculated using Image Pro Plus 6.0 software (Media Cybernetics, Rockville, MD, USA).

Cell Culture

Human corneal epithelial cells (HCECs) were kindly provided by Araki Sasaki Kagoshia (Miyata Eye Clinic, Kagoshima, Japan). Cells were grown in Dulbecco's modified Eagle's medium/F12 (1:1; Invitrogen, Carlsbad, CA, USA) with 10% fetal bovine serum (Invitrogen), and cultured in a 37°C humidified incubator containing 5% CO₂.

SIRT1 Inhibitor Treatment

SIRT1 specific inhibitor ex-527 (Abcam, Cambridge, MA, USA) was dissolved in dimethyl sulfoxide to form a 100 mM stock solution. The effects of ex-527 were evaluated on CEWH at a working concentration of 100 μM diluted by saline solution according to the previous research in vivo.²⁴ Ten microliters ex-527 working solutions were administered topically to the right injured corneas using pipettes every six hours after corneal epithelial debridement. Saline solution treatment of the left injured corneas served as the control. After 24 hours, the recovery of corneal epithelia was examined.

In HCECs, 10 μM ex-527 was added to the cells, and dimethyl sulfoxide treatment was used as the control. After 24 hours treatment, the cells were subjected to further experiments.

Small Interfering RNA (siRNA) Transfection

When HCECs reached 30–40% confluence, the cells were transfected with siRNA mixed with lipofectamine RNAiMAX (Invitrogen). After six hours culture, the medium was replaced with fresh medium. The targeted sequences for the siRNA experiments were as follows: siSIRT1-I: 5'-GAA GTT GAC CTC CTC ATT GT-3', siSIRT1-II: 5'-GTA TTG CTG AAC AGA TGG AA-3'; siCortactin: 5'-GCU GAG GGA GAA UGU CUU U-3'; negative control (NC) siRNA: 5'-UUC UCC GAA CGU GUC ACG UTT-3'.

According to the previous report,⁵ Specific Cortactin or NC siRNA was delivered into the corneal epithelial layer using in vivo-polyethylenimine (Polyplus transfection; ArchiMed, Lyon, France). In brief, the right eyes were intrastromally injected with 100 μM Cortactin siRNA mixed with polyethylenimine using a 33-gauge needle (Hamilton, Bonaduz, Switzerland) under a stereomicroscope; the left eyes were injected with NC siRNA as the control meanwhile. After six hours, corneal epithelial debridement was carried out. The sequences of in vivo siRNA were as follows: siCortactin: 5'-CCA GGA ACA CAU CAA CAU UTT-3'; NC siRNA: 5'-GGC TCT AGA AAA GCC TAT GC-3'. Specific knockdown of SIRT1 or Cortactin was confirmed by Western blot analysis.

In Vitro Scratch Assay

HCECs were seeded in a 12-well plate (Corning, Inc., Corning, NY, USA) and transfected with siRNA. After 48 hours, when the cells were confluent completely, a sterile 100 μL pipet tip was used to form a lengthwise scratch. Floating cells were washed away and replaced with fresh serum-free medium. Images were acquired at zero hours and 24 hours after incubation at the same field using a camera attached to a microscope (100 ×, Axiovert 200; Zeiss, Jena, Germany). The cell migratory behavior is expressed as a percentage of wound closure: Relative Migrated Distance=

$(A_{0h}-A_{24h})/A_{0h} \times 100\%$, A_{0h} and A_{24h} represent the areas of the wound measured at zero hours and 24 hours after scratching, respectively. The wounded areas were evaluated using Image Pro Plus 6.0 software.

Transwell Assay

siRNA-transfected HCECs were trypsinized, resuspended, and replated at a density of 5×10^4 cells/100 μ L in the upper chambers of transwell plates (8 μ m; Corning). Human growth factor 10 ng/mL was added to the medium. After additional 24 hours culture at 37°C, cells were fixed with 4% paraformaldehyde (PFA) for 30 minutes at room temperature (RT), and stained with crystal violet. Cells in the upper chamber were wiped off carefully, and photographs were taken under a phase contrast microscope ($\times 100$; Axiovert 200; Zeiss). Counting cells from five randomly selected areas yielded the average number of cells migrating through the filter. This experiment was repeated three times.

Apoptosis Assay

The apoptotic cells were quantified using terminal deoxynucleotidyl transferase (TdT) deoxyuridine triphosphate (dUTP) nick-end labeling (TUNEL) staining technique. According to the standard protocols of the TUNEL kit (In Situ Cell Death Detection Kit Fluorescein; Roche, Mannheim, Germany), HCECs were plated in triplicate in a 96-well plate (Corning) and transfected with SIRT1 or NC siRNA. After 48 hours, cells were fixed with 4% PFA for one hour. The eyeball sections from eight-week-old mice (the *cKO* or the control mice) were fixed for 20 minutes. After fixing, samples were washed three times with PBS, followed by incubation in permeabilization solution (0.1% triton X-100 in PBS) on ice for two minutes. After washing with PBS three times, samples were incubated with a TUNEL reaction mixture for one hour at 37°C in the dark. Positive controls were performed at the same time by incubating samples with 100 U/mL DNaseI recombinant (Roche). After PBS wash, samples were stained with 4'-6-diamidino-2-phenylindole (DAPI) to label the nucleus, mounted with anti-quenching agents (Sigma-Aldrich, St. Louis, MO, USA), and observed by the confocal microscopy (LSM 710; Zeiss).

Cell Proliferation Assay

The MTS assay kit (CellTiter 96 Aqueous one solution reagent; Promega, Madison, WI, USA) was used to evaluate cell proliferation. HCECs were seeded onto a 96-well plate (Corning) at a density of 3000 per well and transfected with SIRT1 or NC siRNA. After 48 hours' culture, complete medium was removed, a mixture containing 15 μ L MTS and 85 μ L F12 (Invitrogen) was added. The cells were incubated for another two hours. OD values were read at 490 nm using the M5 plate reader (Molecular Devices, San Jose, CA, USA).

Flow Cytometry Analysis

Forty-eight hours after transfection, HCECs were harvested and stained with propidium iodide (Thermo Scientific, Waltham, MA, USA) according to the manufacturer's instructions. DNA content was analyzed with a flow cytometer (FACS caliber; Becton Dickinson, San Jose, CA, USA).

Immunofluorescence Staining

Dissected mouse eyes were embedded in optimal cutting temperature compound (Thermo Scientific) and frozen on liquid nitrogen. The frozen block was cut into 10- μ m-thick sections. Corneal sections and HCECs were fixed in freshly 4% PFA for 30 minutes. After three successive PBS washes, samples were permeabilized with 0.5% TritonX-100 in PBS for 10 minutes and incubated with 5% goat serum in PBS for one hour. The subcellular localization of endogenous SIRT1, Cortactin and acetylated-Cortactin (Ac-Cortactin) was determined by incubating sections with the primary antibodies overnight at 4°C. The Ki67 antibody was used to label the proliferating cells. They were subsequently incubated with fluorescence-conjugated secondary antibodies for one hour in the dark. Antibodies were used as follows: Ac-Cortactin (1:100; EMD Millipore, Seattle, WA, USA), SIRT1 (1:100; Cell Signaling Technology, CST, Beverly, MA, USA), Cortactin (1:200; Abcam), Ki67 (1:100; CST). The sections were washed, stained with DAPI to label nuclei, mounted, and examined by confocal microscopy (LSM 710; Zeiss).

Phalloidin Staining

Twenty-four hours after scratches were made, cells were fixed with 4% PFA for 30 minutes and permeabilized with 0.5% TritonX-100 in PBS for 10 minutes. After being washed three times in PBS, cells were incubated in FITC-Phalloidin (1:100; AAT Bioquest, Pleasanton, CA, USA) to label F-actin for one hour in the dark at RT. The cells were washed and then stained with DAPI, mounted, and examined by confocal microscopy (LSM 710; Zeiss).

Western Blot Analysis

Western blot analysis was performed in accordance with the standard protocol. Total cell lysate was prepared using RIPA lysis buffer (Beyotime Biotechnology, Shanghai, China) with protease inhibitor cocktail. Proteins 20 μ g were loaded and separated by sodium dodecyl sulfate-polyacrylamide gel electrophoresis (SDS-PAGE) gel and electrotransferred to nitrocellulose blotting membranes (0.2 μ m; GE Healthcare Life Science, Uppsala, Sweden). Membranes were incubated with 5% non-fat milk for three hours and incubated with primary antibodies overnight at 4°C. Fluorescence-conjugated secondary antibody (goat anti-rabbit/mouse IRDye; LI-COR Biosciences, Lincoln, NE, USA) diluted in the blocking buffer (1:5000) was incubated for one hour at RT, and protein bands were detected using Odyssey infrared imaging system (LI-COR Biosciences). Primary antibodies were as follows: anti-SIRT1 (1:1000, CST), anti-Cortactin (1:1000; CST), anti-Acetylated-lysine (1:1000; CST), anti-Ac-Cortactin (1:1000; Millipore), anti-Histone3 (H3; 1:1000; CST) anti-Ac-H3 (1:1000; Millipore), anti-Histone4 (H4; 1:1000; CST), anti-Ac-H4 (1:1000; Millipore), anti- β -Actin (1:1000; CST). The protein bands were analyzed by Image J (NIH) software.

Co-Immunoprecipitation

Co-Immunoprecipitation was performed according to the standard procedures provided in the Pierce Classic IP Kit (Thermo Scientific). Briefly, cells were lysed in IP lysis buffer (Thermo Scientific) added with a protease inhibitor cocktail. Cell lysates underwent incubation with primary antibodies

overnight at 4°C. Targeted immune complex was captured using protein A/G agarose and eluted with elution buffer. Antibodies used for IP were as follows: anti-SIRT1 (1:100; CST), anti-Cortactin (1:100; Millipore), and anti-IgG (1:100; Millipore). Immunoprecipitates were subjected to SDS-PAGE as described above.

Mass Spectrometry Analysis

Protein was obtained by IP using an anti-SIRT1 antibody and loaded onto SDS-PAGE. The separated protein bands stained by Coomassie blue were excised from the gel and subjected to mass spectrometry (MS) performed by the Chinese Academy of Sciences, Shanghai. Briefly, Experiments were performed on a Q Exactive mass spectrometer (Thermo Scientific) that was coupled to an Easy nLC1000 HPLC system. A data-dependent top-10 method was adopted to acquire MS data, choosing the most abundant precursor ions from the survey scan (resolution of 70,000 at 200 m/z). Protein Discoverer software (version 1.1; Thermo Scientific) was used to process the raw data. A UniProt database of *Synechocystis* 6803 proteins was searched using an in-house Mascot server (version 2.2). One missed trypsin cleavage, Met oxidation, 6-ppm, and 0.1-D mass accuracies for the mass spectrometry and tandem mass spectrometry modes, were all allowed under the search criteria, respectively.

Quantitative Reverse Transcription Polymerase Chain Reaction

Cells were lysed in Trizol reagent according to the manufacturer's instructions. Each RNA extract (1 µg) was reverse transcribed into cDNA by using the reverse transcription system kit (Promega, Madison, WI, USA). Quantitative reverse transcription polymerase chain reaction (RT-qPCR) was performed using an ABI ViiA7 real-time PCR system (Thermo Scientific). Amplification and quantification were performed in a 20 µL reaction mixture containing 10 µL Power SYBR Green PCR master mix (Thermo Scientific), 1 µL cDNA, 1 µL primers, and 8 µL ddH₂O. The reaction condition was as follows: 50°C for two minutes; 95°C for 10 minutes; 40 cycles of 95°C for 15 seconds, and 60°C for 60 seconds. A *β-Actin* was used as an internal control for gene expression normalization. The data were analyzed and expressed as relative gene expression using the $2^{-\Delta\Delta CT}$ method. The sequences of the PCR primers are presented in the supplementary data (Supplementary Table).

Statistical Analysis

All data are provided as mean ± standard error of the mean. Difference between two groups was tested by a two-sided Student *t* test. $P < 0.05$ was referred as statistically significant. Statistical significance: * $P < 0.05$; ** $P < 0.01$; *** $P < 0.001$.

RESULTS

Acetylated Lysine Profiles and Expression of SIRT1 during Corneal Epithelial Wound Healing

To determine whether acetylation modification occurs in the corneal epithelia during CEWH, we compared the level of lysine-acetylated proteins in the harvested CE during wound healing with that in the basal condition using West-

ern blotting. The result indicated that the level of acetylated lysine in non-histone proteins decreased significantly during CEWH. Interestingly, the level of acetylated-histones instead was up-regulated (Fig. 1A). These opposing effects were further confirmed by Western blot assay using anti-acetylated-Histone3 (Ac-H3) and anti-acetylated-Histone4 (Ac-H4) antibodies. The result showed that both Ac-H3 and Ac-H4 significantly increased in WH corneal epithelia (Fig. 1B). Next, we tested the mRNA profiles of acetylase and deacetylase by RT-qPCR analysis. The respective expression levels of acetylases *Kat1* and *Kat2b* increased, whereas *Kat6b* and *Kat13a-c* decreased in the WH samples compared with the control counterparts (Fig. 1C). Among the HDACs, *Sirt1* was upregulated almost threefold (Fig. 1D). Western blot analysis verified a near twofold upregulation of Sirt1 during CEWH (Fig. 1E). Taken together, the lysine-acetylated protein profiles during CEWH suggest that increased Sirt1 expression levels may account for the decreases in acetylated non-histone proteins, which may contribute to regulating CEWH.

Generation of Corneal Epithelial-Specific *Sirt1* Deletion Mice

To determine the function of *Sirt1* in the corneal epithelia, we conditionally inactivated *Sirt1* in the corneal epithelia using *Krt12-Cre* and *Sirt1^{fllox/fllox}* mice to generate *Sirt1* conditional knockout (*cKO*) mice (Figs. 2A, 2B). The morphology and thickness of corneal epithelia showed no overt phenotype in *cKO* mice compared with their counterparts (Supplementary Fig. S1). To determine whether *Krt12-Cre*-mediated ablation of *Sirt1* was successful, we collected corneal epithelia and then performed Western blotting to analyze *Sirt1* protein expression. *Sirt1* protein expression was absent in the *Sirt1 cKO* CE compared with the control counterparts (Fig. 2C). Immunofluorescent staining further confirmed that *Sirt1* was absent in the nucleus of the *cKO* corneal epithelia compared with the controls (Fig. 2D).

Corneal Epithelial-Specific *Sirt1* Deletion Delays Corneal Epithelial Wound Healing In Vivo

To determine whether epithelial *Sirt1* expression contributes to mediating CEWH, we used an in vivo eight-week-old model of CEWH. A 2.0-mm corneal epithelial debridement wound was created in the *cKO* and the control mice. Twenty-four hours after injury, *cKO* mice had a larger wound area than their control counterparts. The wound area was $43.2\% \pm 1.5\%$ in the *cKO* mice compared with $28.5\% \pm 2.0\%$ in the *Sirt1^{fllox/fllox}* mice and $20.0\% \pm 4.5\%$ in the *Krt12-Cre* mice. The control mice had totally healed 48 hours after damage, whereas the *cKO* mice still had $13.2\% \pm 2.3\%$ wound area (Figs. 3A, 3B). To validate *Sirt1* activity involvement, the effect of the *Sirt1* specific inhibitor ex-527 was evaluated during CEWH. Ex-527 treatment inhibited CE repair significantly compared with saline treatment (Figs. 3C, 3D). Immunostaining with ki67 was used to detect the proliferative behavior of the CE. The result showed no apparent difference in the number of Ki67-positive cells between the *cKO* and the control mice (Figs. 3E, 3F). This lack of difference implies that *Sirt1* deletion causes CEWH declines primarily by affecting migration. Altogether, these findings imply that CEWH was suppressed by *Sirt1* deletion in CE owing to decreased migration rather than proliferation.

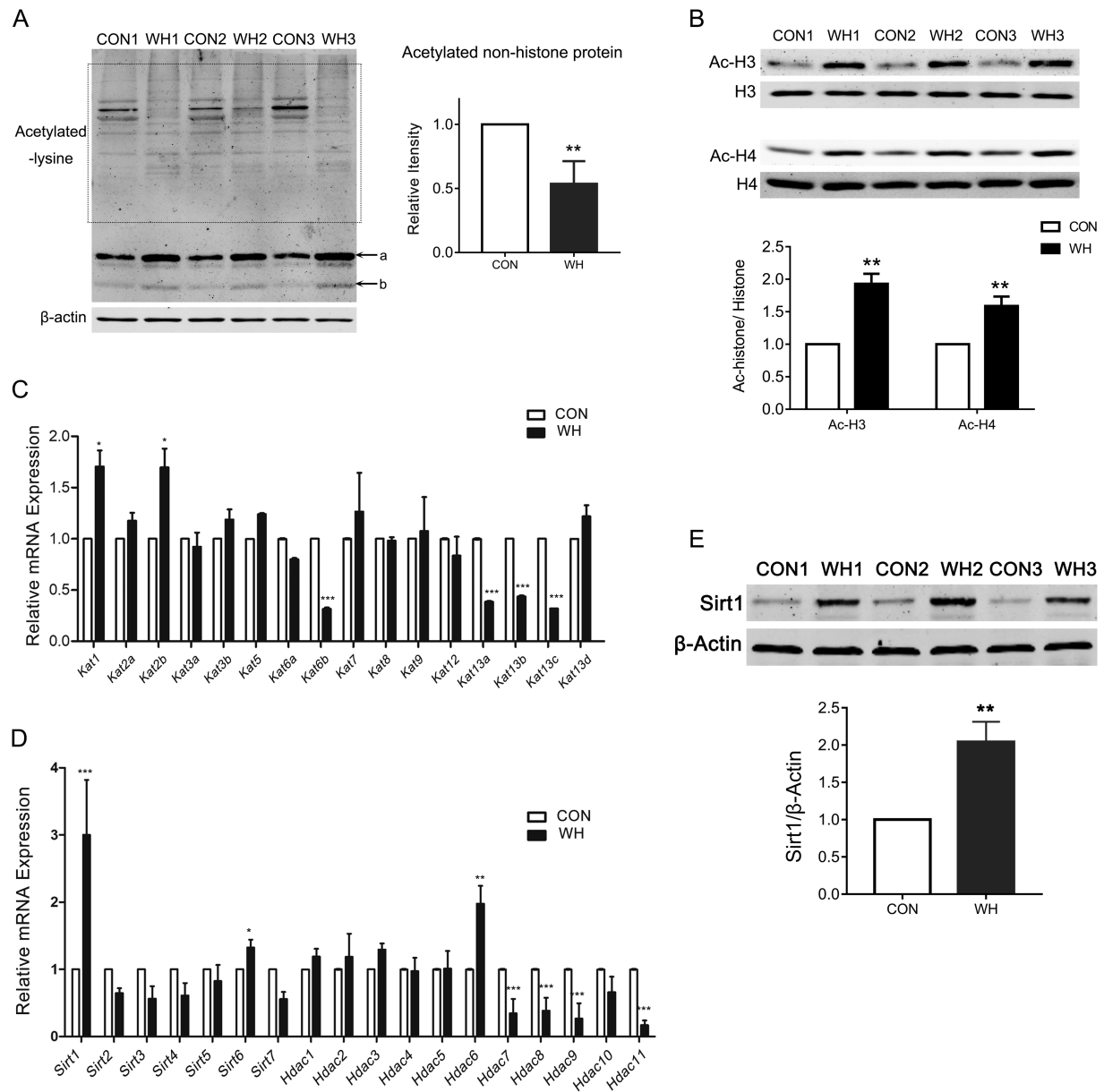


FIGURE 1. Acetylated-lysine profiles in the re-epithelialized cornea epithelia. **(A)** CE was collected as the control group. At 48 hours after wounding, the CE was completely healed and collected as the wound healing (WH) group. Western blot assay determined the level of lysine-acetylated proteins in WH groups ($n = 6$ /group) compared with the controls. The bands a, b were supposed to be acetylated-histone 3 and acetylated-histone 4, respectively. The densitometry of the levels of lysine-acetylated non-histone proteins (*dashed box*) was quantified. CON, control corneas. **(B)** Western blot images and histograms of densitometry of acetylated-histone 3 (Ac-H3) and acetylated-histone 4 (Ac-H4) in the wound healing corneal epithelia and the control corneas ($n = 6$ /group). Histone 3 (H3) and Histone 4 (H4) were used as internal references. **(C)** RT-qPCR detected the lysine acetyl-transferases (KATs) and **(D)** histone deacetylases (HDACs) mRNA expression levels in the WH epithelia and those in the control corneas ($n = 4$ /group). **(E)** Western blot images and quantification of densitometry of Sirt1 protein expression in the re-epithelial cells collected during CEWH compared with those in the control epithelia ($n = 6$ /group). The β -actin was used as the internal reference.

SIRT1 Knockdown Inhibits Human Corneal Epithelial Migration In Vitro

SIRT1 siRNA transfection was further performed to determine whether loss of SIRT1 function inhibited human corneal epithelial migration. Two sets of siRNAs targeting different regions of the SIRT1 transcript were used to avoid the off-target effect. The SIRT1 protein expression level

was reduced by 80% in the siSIRT1 transfected cells relative to the NC siRNA transfected HCEC (Supplementary Fig. S2). The scratch wound assay revealed that healing was 40% slower than the NC transfected cells after 24 hours, which is statistically significant (Figs. 4A, 4B). In addition, we further investigated the specific effect of SIRT1 on cell migration using the transwell assay. The result showed that fewer cells migrated through the transwell membrane in

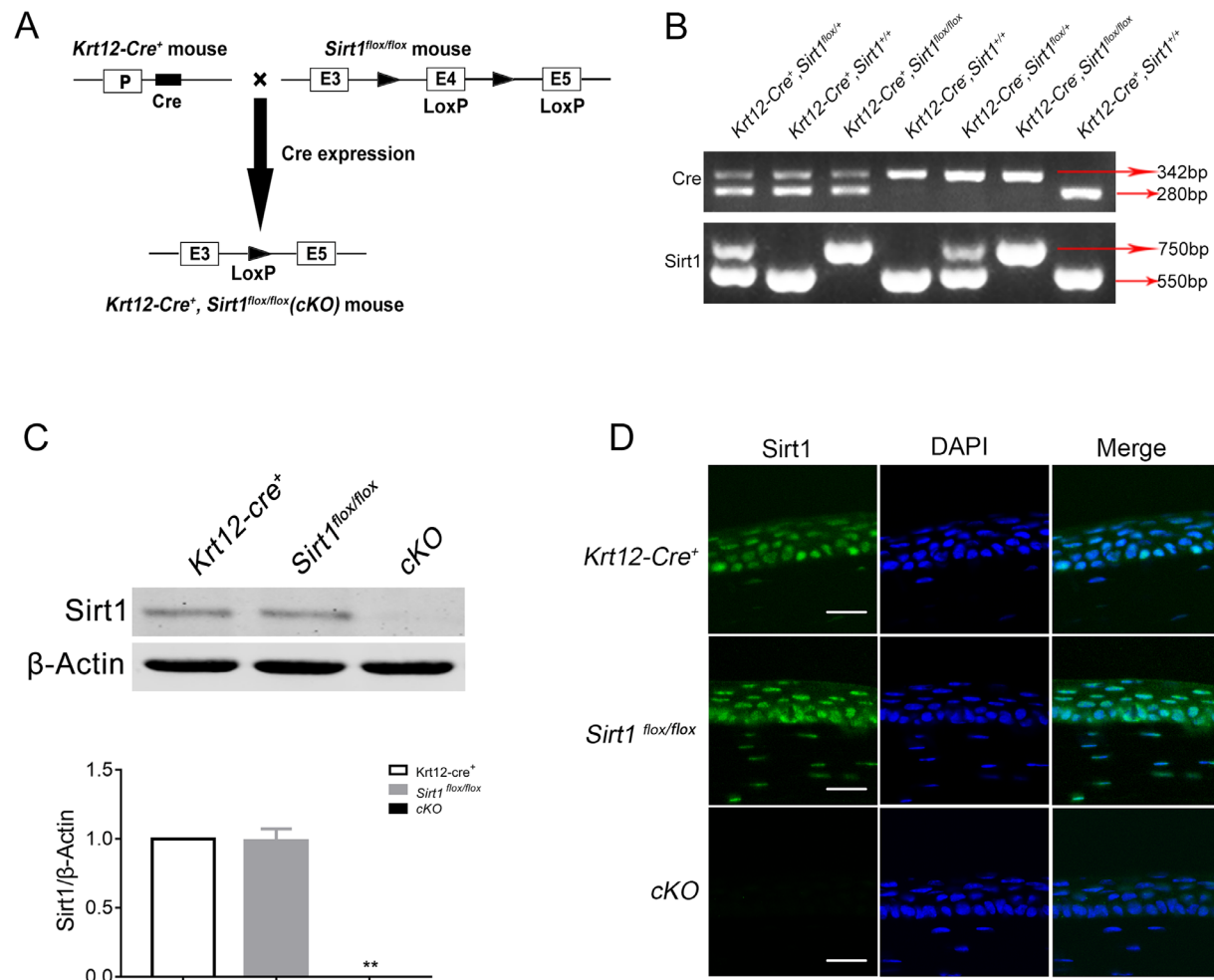


FIGURE 2. Generation of corneal epithelial-specific *Sirt1* knockout mice. (A) Strategy to generate CE-specific deletion of *Sirt1* gene in mice. Conditional *Sirt1* allele was generated by inserting *loxP* sites flanking exon 4 of mouse *Sirt1* genomic locus. CE-specific *Sirt1* deletion mice were obtained by breeding with *Krt12-Cre* transgenic mice. (B) Genotype identification of CE-specific *Sirt1* deletion mice by PCR. *Krt12-cre*⁻, *Sirt1*^{+/+}: wild type mice; *Krt12-cre*⁻, *Sirt1*^{lox/lox}: *Sirt1* heterozygous mice; *Krt12-cre*⁻, *Sirt1*^{lox/lox/lox}: *Sirt1* homozygous mice; *Krt12-cre*⁺, *Sirt1*^{+/+}: *Krt12-Cre* mice; *Krt12-cre*⁺, *Sirt1*^{lox/lox}: CE-specific *Sirt1* deletion heterozygous mice; *Krt12-cre*⁺, *Sirt1*^{lox/lox/lox}: CE-specific *Sirt1* knockout (cKO) mice. (C) Western blot analysis and quantification of Sirt1 in corneal epithelia showed efficient depletion of Sirt1 in the cKO mice compared with the controls (n = 4/group). (D) Representative immunofluorescence micrographs of Sirt1 in corneal cryosections of the *Sirt1* cKO mice and the controls (Green, Sirt1; Blue, DAPI). Scale bars: 50 μ m.

the SIRT1 knockdown group compared with the control group (Supplementary Fig. S3). The effect of SIRT1 knockdown on cell proliferation was analyzed based on an MTS assay. The result showed that both the siSIRT1 transfected and the siNC transfected cells had identical proliferation rate (Fig. 4C). Flow cytometry analysis further showed that the inhibition of SIRT1 expression had no significant effects on the cell cycle distribution profiles compared with the NC group (Figs. 4D, 4E). Furthermore, we determined the effect of SIRT1 knockdown on corneal epithelial cell apoptosis using TUNEL assay. The results showed no apoptotic cells were detected in both siSIRT1 and NC transfected HCECs (Supplementary Fig. S4A). We also examined the apoptosis of CE in the SIRT1 cKO and the control mice. TUNEL analysis showed no significant difference in apoptotic rate of the corneal epithelia (Supplementary Fig. S4B). Taken together, these results confirmed that loss of SIRT1 function selectively inhibited cell migration.

SIRT1 Binds and Deacetylates Cortactin in HCECs

To gain insight into how SIRT1 regulates HCEC migration, we performed MS to screen the proteins interacting with SIRT1. Cortactin, an actin-binding protein, is among the highly expressed proteins (Fig. 5A). To determine whether SIRT1 associates with cortactin, we assessed cortactin and SIRT1 localization in HCECs by Co-immunostaining. The result showed that cortactin was distributed in the nucleus and cytoplasm, and SIRT1 and cortactin co-localize with one another in the nucleus (Fig. 5B). In addition, co-IP analysis performed by using an anti-SIRT1 antibody followed by Western blot with an anti-Cortactin antibody revealed that SIRT1 interacted with cortactin (Fig. 5C). Their association with one another was confirmed by reciprocal co-IP using an anti-Cortactin antibody followed by Western blot with an anti-SIRT1 antibody (Fig. 5D). Next, we examined whether SIRT1 can regulate the cortactin acetylation

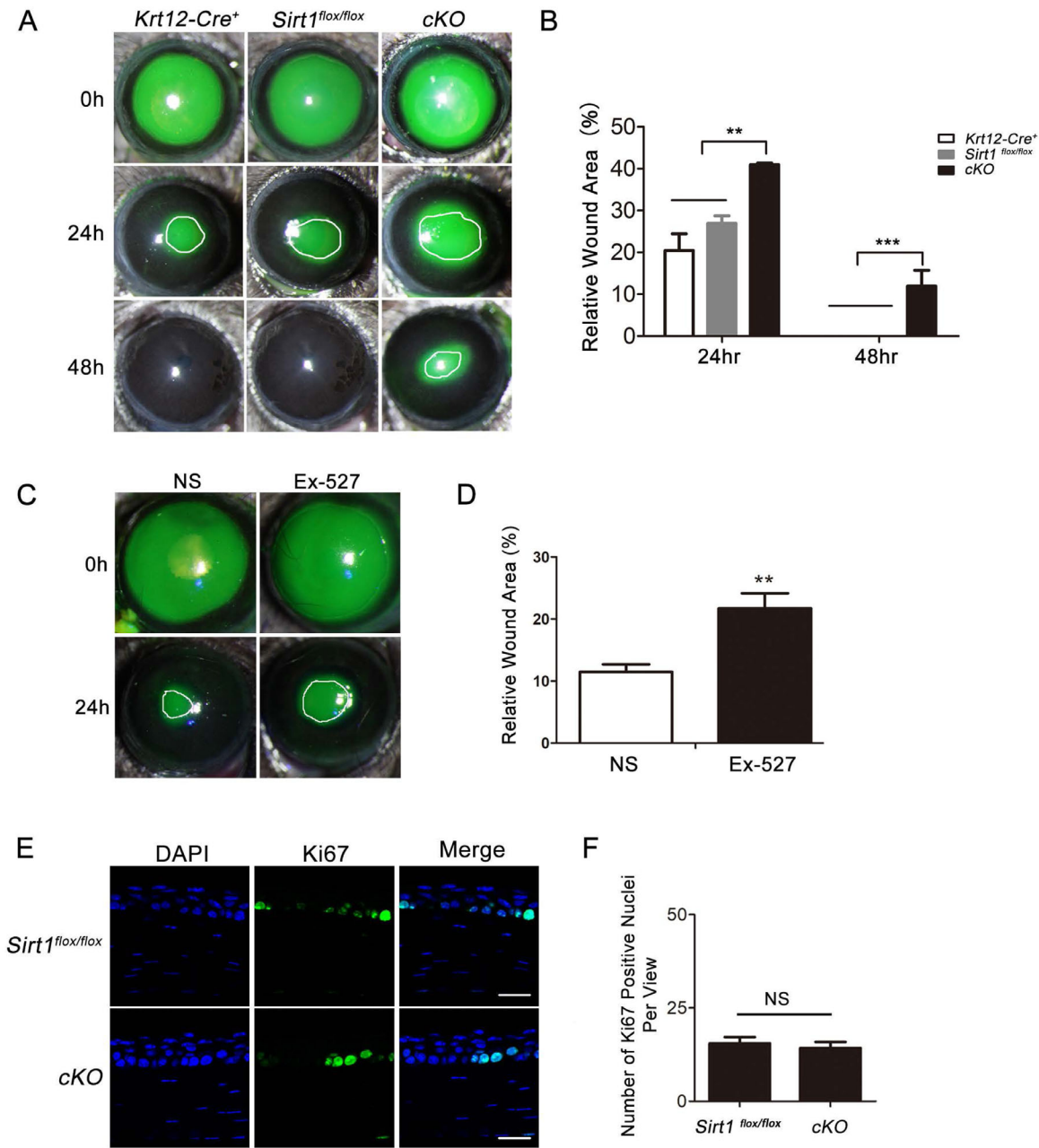


FIGURE 3. *Sirt1* deletion in the corneal epithelia delays CEWH. (A) Representative photographs and (B) quantification of fluorescein staining scratches in the *cKO* and the control mouse corneas at zero hours, 24 hours, and 48 hours after corneal epithelial injury ($n = 6$ /group). (C) Representative photographs and (D) quantification of fluorescein-positive staining scratched areas in the ex-527 treated corneas and the control corneas (normal saline-treated) at zero hours and 24 hours after corneal epithelial injury ($n = 6$ /group). NS, normal saline solution. (E) Representative images and (F) quantification of Ki67 immunofluorescence in the mouse corneal cryosections at 48 hours after corneal injury in the *Sirt1* *cKO* mice and the control counterparts ($n = 6$). NS, no significant difference.

status. As shown in Figure 5E, the immune-staining of Ac-Cortactin in the nuclei of siSIRT1 transfected HCECs was more potent than that of siNC transfected cells. We also examined the protein expression levels of the total Cortactin and Ac-Cortactin in the siSIRT1 transfected HCECs. The total cortactin protein expression level was unaffected by SIRT1 downregulation. However, the Ac-Cortactin expression level increased in a certain degree in the siSIRT1 transfected HCECs (Figs. 5F, 5G). To confirm the impact of the loss of SIRT1 activity on Ac-Cortactin level, we treated HCECs with 10 μ M ex-527. As expected, the Ac-Cortactin

protein level increased significantly in the ex-527 treated HCECs (Supplementary Fig. S5). Furthermore, the intensity of Ac-Cortactin immunostaining in nuclear was substantially greater in the *cKO* mice, as compared to that in the control mice. While there was no significant difference in total cortactin staining intensity (Fig. 5H). Western blot assay results also confirmed the higher Ac-Cortactin protein expression levels in *cKO* mice (Fig. 5I). Altogether, these data suggest that SIRT1 binds to and deacetylates cortactin in the corneal epithelia both in vivo and in vitro.

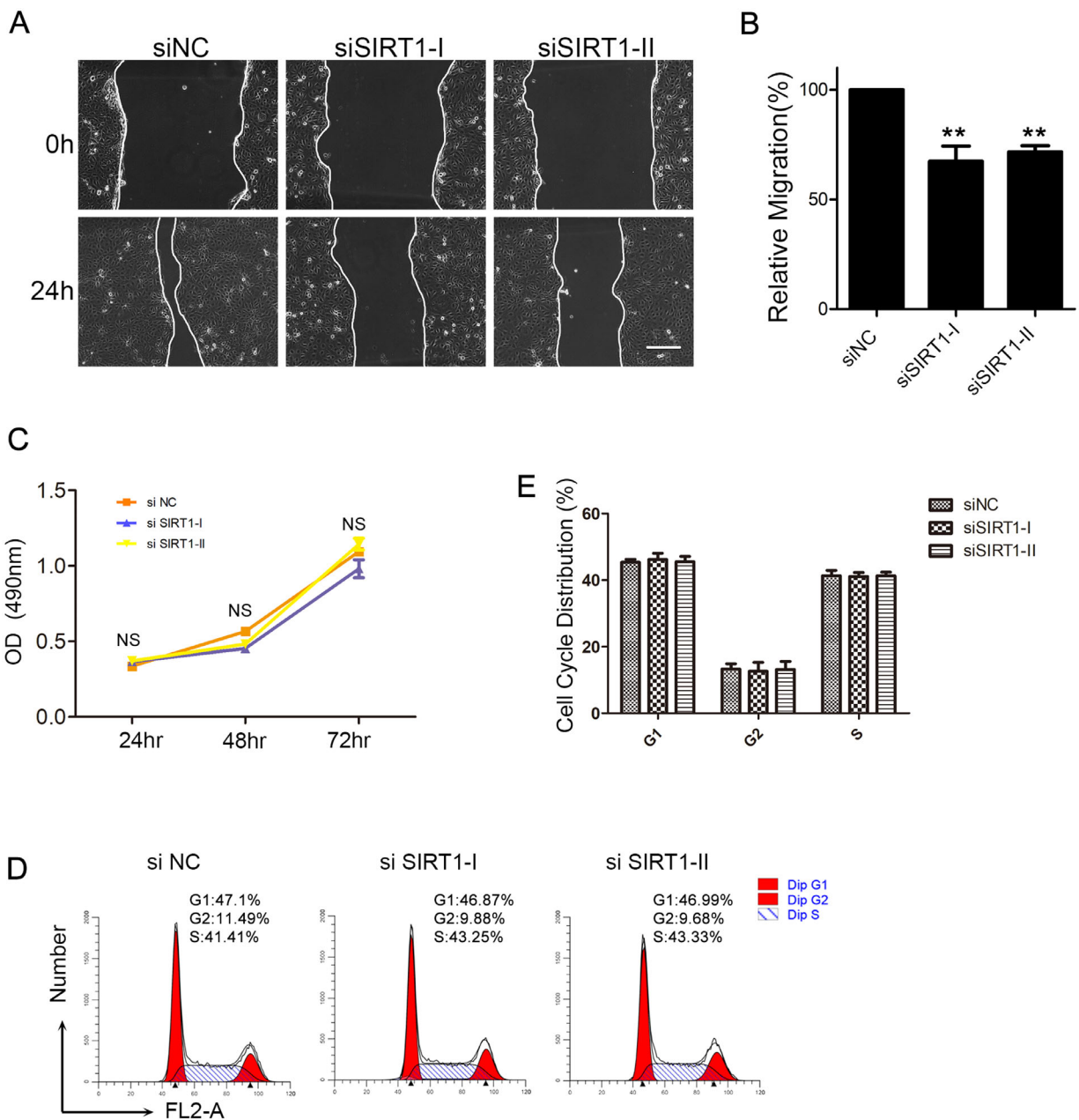


FIGURE 4. SIRT1 Knockdown inhibits HCEC migration rather than proliferation. **(A)** Representative phase-contrast images of the initial wound (0 h) and 24 hours after scratch wound in the siSIRT1 transfected and the control HCECs. *Scale bars:* 200 μ m. **(B)** Quantification of the percentage of the initial wound at 24 hours after scratch wound ($n = 3$ /group). **(C)** MTS assay analyzed the effect of SIRT1 downregulation on the proliferation of HCECs ($n = 3$ /group). NS, no significant difference. **(D)** Flow cytometry analyzed the effect of SIRT1 downregulation on the cell cycle distribution. **(E)** Statistical analysis of the cell cycle distribution in the siSIRT1 transfected HCECs compared to the control cells ($n = 3$ /group).

Cortactin Inhibition Suppresses Migration Because of Decreased Formation of Lamellipodia in Corneal Epithelia

As previously reported, the acetylation of cortactin rendered it inactive.²⁵ To simulate this effect, we transfected HCECs with cortactin siRNA to inactivate the protein (Supplementary Figs. S6A, S6B). Scratch assay results showed that the cortactin siRNA transfected HCECs migrated 35% slower than the NC group (Figs. 6A, 6B). The role of cortactin expression in modulating CEWH in vivo was

further investigated using Cortactin siRNA injection in corneal epithelia (Supplementary Figs. S6C, S6D). Similar to its effect in vitro, CEWH was retarded by 50% in the cortactin siRNA injected mice (Figs. 6C, 6D). The effects of either cortactin or SIRT1 downregulation on actin cyto-architecture were studied using FITC-phalloidin labeling. As shown in Figure 6E, either cortactin or SIRT1 knockdown reduced the formation of lamellipodia and marginal actin bundles in HCECs at the wound edge, which resulted in decreased migration.

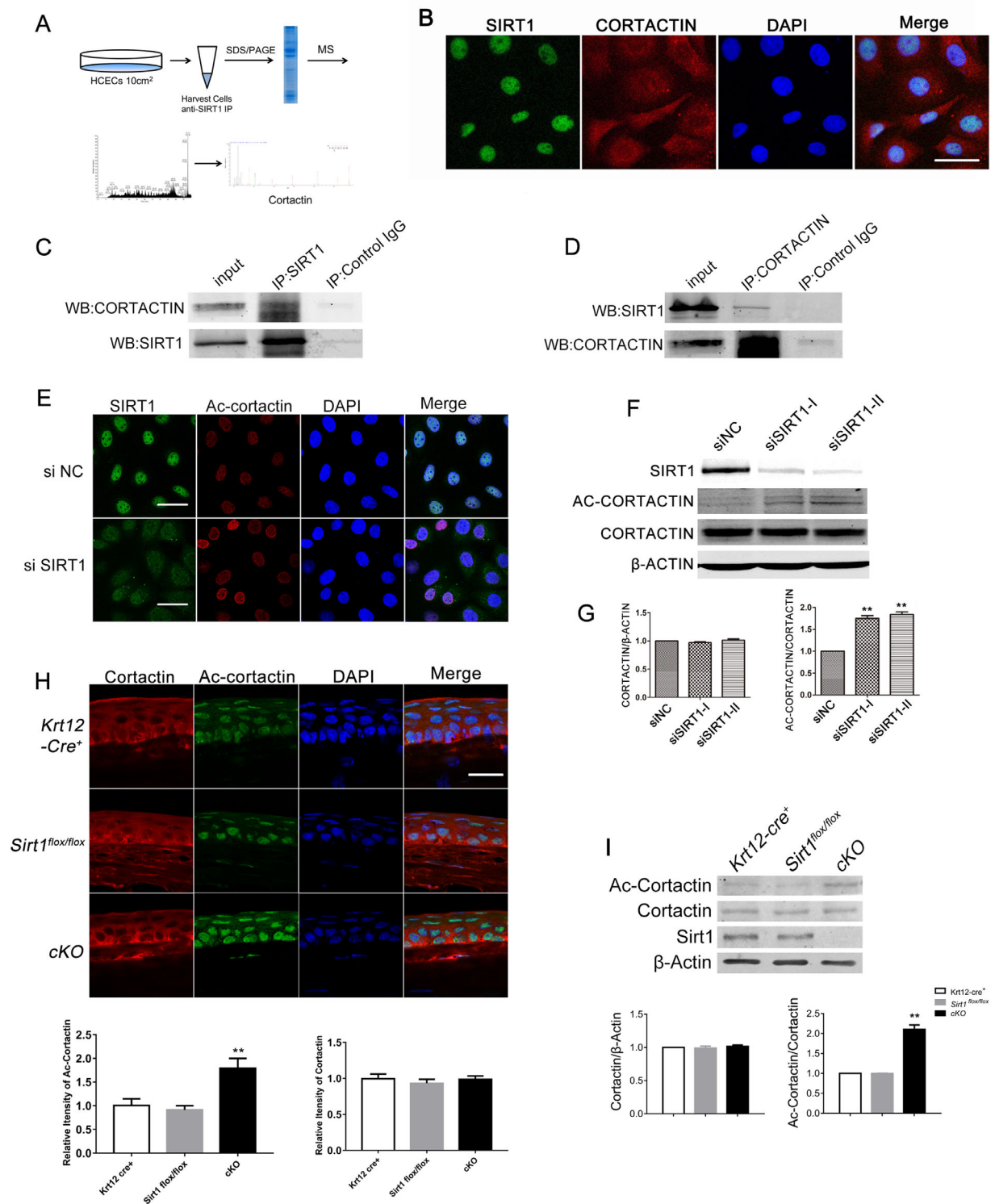


FIGURE 5. SIRT1 deacetylates Cortactin in corneal epithelial cells. **(A)** Diagrammatic representation of the workflow used to analyze the interacting proteins with SIRT1 in HCECs using mass spectrometry analysis. **(B)** Immunofluorescence evaluation of SIRT1 (green) and endogenous Cortactin (red) expression in HCEC. The nucleus was stained with DAPI (blue). Representative green, red, blue, and merge images ($\times 400$) captured on a confocal microscope are shown. Scale bars: 50 μ m. **(C)** Representative images of the immunoprecipitation bands. After immunoprecipitation of cell lysates with anti-Sirt1 antibody, the immunoprecipitants were immunoblotted with an anti-Cortactin antibody. Immunoprecipitants with IgG were used as controls. **(D)** After immunoprecipitation of cell lysates with anti-Cortactin antibody, the immunoprecipitants were immunoblotted with an anti-SIRT1 antibody. Immunoprecipitants with IgG were used as controls. **(E)** Representative immunofluorescence images showed that the fluorescence intensity of Ac-cortactin in the siSIRT1 transfected HCECs was more potent compared with the control counterpart. Scale bars: 50 μ m. **(F)** Western blotting analyzed the protein levels of Ac-cortactin and the total cortactin in the siSIRT1 transfected HCECs. **(G)** Quantification of densitometry of the protein levels of Ac-cortactin and the total cortactin in the siSIRT1 transfected cells ($n = 3/\text{group}$). **(H)** Representative immunofluorescence images of mouse corneal cryosections and statistical

analysis showed the fluorescence intensity of Ac-cortactin in the *Sirt1* cKO was stronger compared with the control counterparts (*Krt12-cre⁺* and *Sirt1^{fllox/fllox}* mice), while there is no alteration of the intensity of Cortactin ($n = 6/\text{group}$). (I) Western blotting analyzed protein levels of Ac-cortactin and the total cortactin in the cKO corneal epithelia and the control corneas, and the densitometry of the protein levels of Ac-Cortactin and the total Cortactin was quantified ($n = 3/\text{group}$).

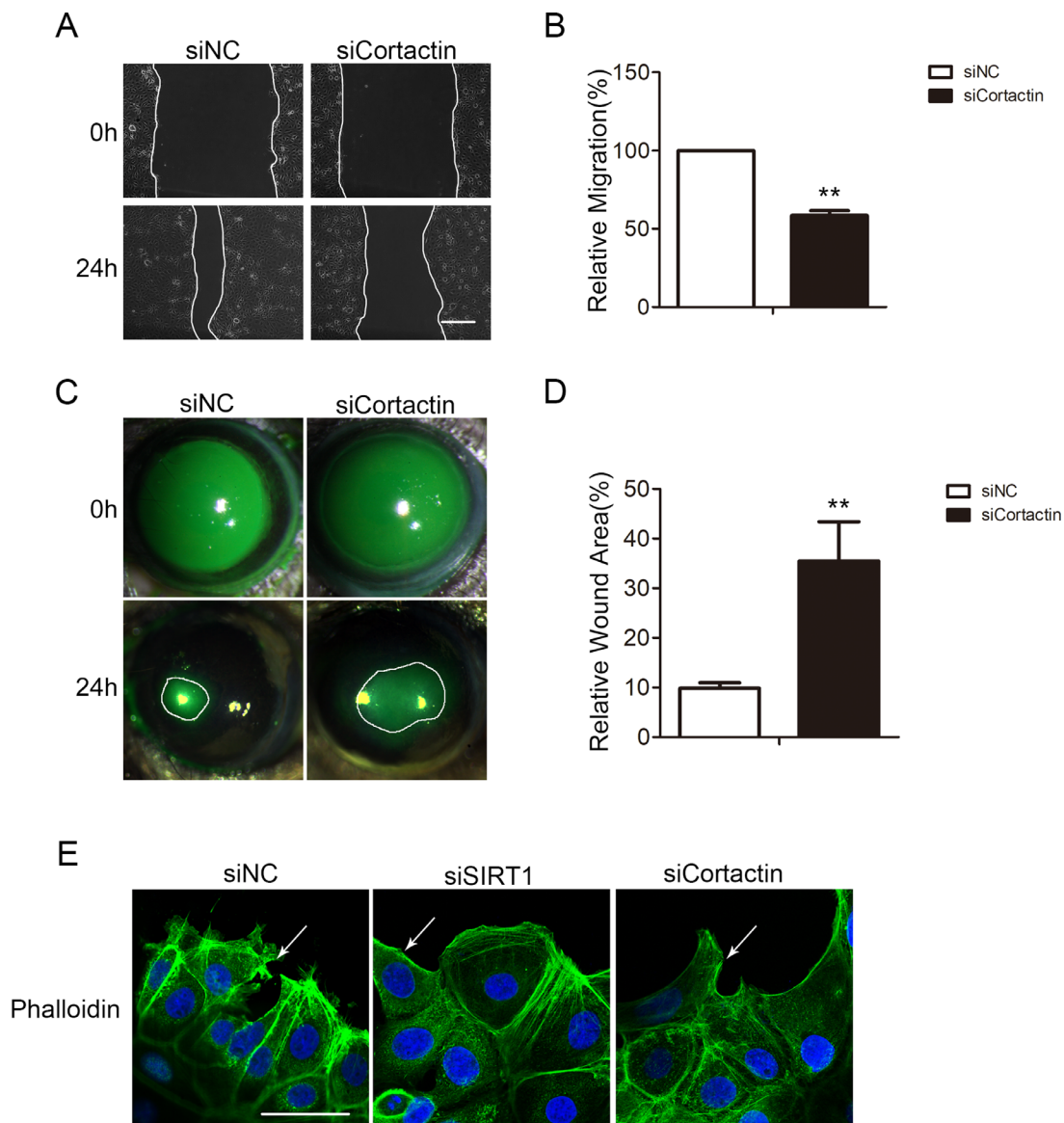


FIGURE 6. Cortactin decline elicits the same phenotype as SIRT1 ablation in the corneal epithelia. (A) Representative phase-contrast images of the initial wound (0 h) and at 24 hours after scratch wound in the siCortactin transfected and the control HCECs. *Scale bars:* 200 μm . (B) Quantification of the percentage of the initial wound area at 24 h after a scratch wound ($n = 3/\text{group}$). (C) Representative photographs and (D) Quantification of corneal wound areas in the siCortactin injected corneas and the control corneas at zero hours and 24 hours after corneal epithelial abrading ($n = 6/\text{group}$). (E) FITC-phalloidin (green) staining of cells at the wound margin showed polymerization of F-actin and formation of lamellipodia (arrows) along the wound edge. Cells were stained with FITC-phalloidin (green) to detect actin filaments, with DAPI (blue) to detect nuclei. *Scale bars:* 50 μm .

DISCUSSION

In eukaryotes, lysine acetylation is a reversible and dynamic post-translational modification that affects hundreds of histones and non-histone proteins. Changes in acetylation status modulate numerous responses associated with different physiological and pathophysiological responses,

such as cancers,²⁶ metabolic diseases,²⁷ and cardiovascular disorders.²⁸ In the current study, the acetylation status of histone3 and histone4 increased during CEWH. Consistent with these effects, several studies showed that increases in histone acetylation levels promoted re-epithelialization after skin wounding.^{29,30} Histone acetylation has been shown to improve gene transcription in most instances,¹² which

might aid corneal epithelial migration to heal. Interestingly, we found for the first time that the acetylation status of non-histone proteins instead decreased during this process. Acetylation modification enhances or suppresses the activity of proteins depending on the acetylated site.²⁶ Here, deacetylated proteins possibly activate proteins to assist CEWH. Elevated deacetylase or declined acetylase leads to a decrease in protein acetylation. In the current study, among these deacetylases that maintain the balance of acetylation status, SIRT1, SIRT6, and HDAC6 were increased during CEWH. SIRT6³¹ and HDAC6³² were previously reported to play essential roles in maintaining corneal homeostasis. Consistent with our group's previous findings,⁶ SIRT1 was shown to be significantly upregulated in the CEWH process, indicating it is responsible for the downregulation of the acetylation level of proteins. Taken together, SIRT1 control of the acetylation state of proteins appears to be critical for maintaining proper CEWH.

Sirtuins, a family of NAD⁺ dependent histone deacetylase, contains seven members (SIRT1-7) with diverse functions in mammals.³³ Emerging evidence indicates that sirtuins are involved in promoting corneal epithelial wound healing. Specifically, Sirt3 promotes diabetic corneal epithelial wound repair by regulating mitophagy levels.³⁴ In addition, Sirt6 deficiency resulted in corneal keratitis and opacity, which hampered corneal epithelial wound healing.³¹ To discover the precise role of SIRT1 in the CEWH process, we established CE-specific *Sirt1* knockout mice. Such *cKO* mice showed no histological abnormalities in adult corneas. However, corneal epithelial wound healing was dramatically retarded. The role of SIRT1 activity was further confirmed by showing that the SIRT1 inhibitor ex-527 also retarded epithelial wound healing. In agreement with our findings, epidermis-specific deletion of *Sirt1* reduced epidermal healing by inhibiting cell migration and inflammation, suggesting SIRT1 activation enhances the epidermal repair process.¹⁹ Proliferation and migration are the key steps during the CEWH process. Hence, we determined whether the number of Ki67-positive cells differed between the *Sirt1* cKO corneas and the controls during CEWH. Interestingly, *Sirt1* deletion did not affect the proliferation of corneal epithelial cells. Like our previous study, SIRT1 affects migra-

tory behavior other than proliferation in human retinal endothelial cells.³⁵ In summary, *Sirt1* deficiency suppressed CEWH solely because of declined migration.

We further explored the impact of SIRT1 on HCECs to confirm whether the insights gained from the *Sirt1* cKO mice can be applied to humans. Consistent with the *in vivo* findings, SIRT1 down-regulation dramatically decreased HCEC migration rather than proliferation. SIRT1 is involved in a myriad of cellular processes, such as proliferation, differentiation, angiogenesis, and migration. Loss of SIRT1 activity has been shown to limit migration in endothelial cells,³⁵ as well as a variety of cancer cells.^{36,37} In the present study, SIRT1 has a strong influence on corneal epithelial migration, probably because of SIRT1's specific modulation of proteins whose acetylation state is entirely responsible for CEC movement. Future research should define which proteins are SIRT1's downstream targets during CEWH, based on the varied impacts of SIRT1 on these responses.

A critical observation in our study is that SIRT1-mediated Cortactin deacetylation contributes to mediating wound-induced increases in corneal epithelial migration. Our current study showed that Cortactin is abundantly bound to SIRT1 in HCECs. Cortactin is functionally entailed in a variety of cellular processes relating to structures. It contains highly conserved F-actin binding repeats, which could be acetylated to regulate its activity.³⁸ Acetylation of Cortactin neutralizes charged lysine residues within the binding domain of F-actin, thereby abrogating the Cortactin binding to F-actin and decreasing cell motility.³⁹ In this study, acetylated Cortactin was found mainly in the CE nucleus, and its amount was shown to be negatively associated with SIRT1 expression. Considered together with the findings that SIRT1 is co-precipitated with Cortactin, and it is co-localized with acetylated-Cortactin in the nucleus, SIRT1 is necessary for the cytoplasmic distribution of Cortactin. In addition, we confirmed the role of Cortactin in CEWH by showing that decrease of Cortactin significantly slowed corneal epithelial migration *in vivo* and *in vitro*. This anti-migration impact is congruent with the previous findings in podocytes⁴⁰ and GnRH neurons,⁴¹ whose cyto-architecture maintenance are dependent on Cortactin deacetylation by SIRT1. The first step in cell movement involves the formation

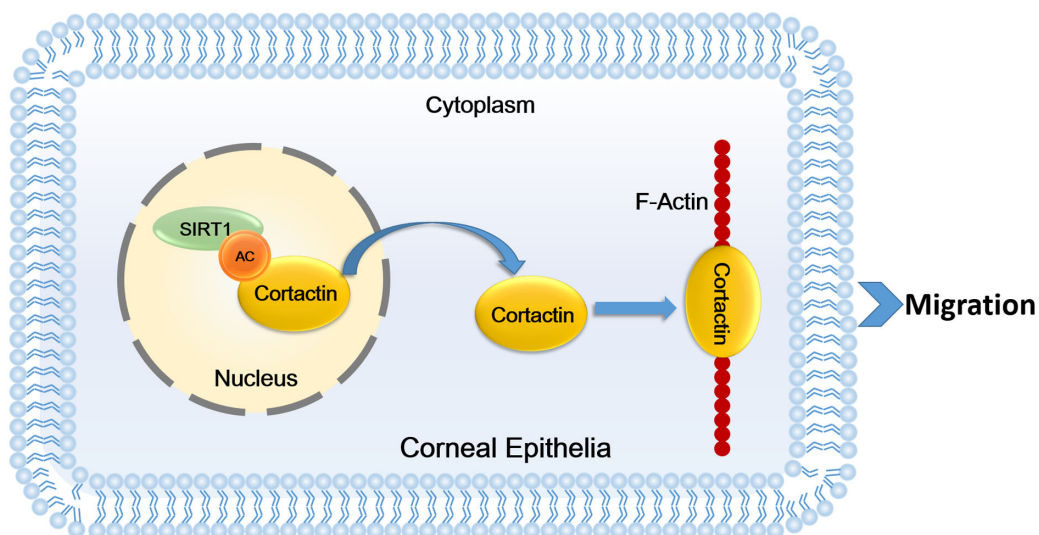


FIGURE 7. Schematic representation of SIRT1 regulation through deacetylating Cortactin during corneal epithelial migration.

of lamellipodial protrusions, which are cytoskeletal protein actin projections at their leading edges.⁴² Loss of SIRT1 function decreased the lamellipodial protrusions, mimicking the inhibitory effect of loss of Cortactin function on cell migration. Taken together, SIRT1-mediated deacetylation of Cortactin promotes lamellipodial formation and in turn increases cell migration during CEWH.

In conclusion, increases in Cortactin acetylation status resulting from loss of SIRT1 function suppress CEWH through decreased lamellipodia formation at the wound edges of migrating cells (Fig. 7). Strategies to promote the SIRT1-Cortactin signaling axis may prove to be an effective therapeutic approach to enhancing CEWH.

Acknowledgements

Supported in part by the National Natural Science Foundation of China (NSFC, No. 81900818, No. 81700801), Natural Science Foundation of Zhejiang Province (No. LY21H120005).

Disclosure: **Y. Lin**, None; **Q. Liu**, None; **L. Li**, None; **R. Yang**, None; **J. Ye**, None; **S. Yang**, None; **G. Luo**, None; **P.S. Reinach**, None; **D. Yan**, None

References

1. Yu FS, Yin J, Xu K, Huang J. Growth factors and corneal epithelial wound healing. *Brain Res Bull.* 2010;81:229–235.
2. Yoshioka R, Shiraishi A, Kobayashi T, et al. Corneal epithelial wound healing impaired in keratinocyte-specific HB-EGF-deficient mice in vivo and in vitro. *Invest Ophthalmol Vis Sci.* 2010;51:5630–5639.
3. Yanai R, Nishida T, Hatano M, et al. Role of the neurokinin-1 receptor in the promotion of corneal epithelial wound healing by the peptides FGLM-NH2 and SSSR in neurotrophic keratopathy. *Invest Ophthalmol Vis Sci.* 2020;61:29.
4. Luo G, Jing X, Yang S, et al. DNA methylation regulates corneal epithelial wound healing by targeting miR-200a and CDKN2B. *Invest Ophthalmol Vis Sci.* 2019;60:650–660.
5. Yang S, Chen W, Jin S, et al. SUV39H1 regulates corneal epithelial wound healing via H3K9me3-mediated repression of p27. *Eye Vis (Lond).* 2022;9:4.
6. An J, Chen X, Chen W, et al. MicroRNA expression profile and the role of miR-204 in corneal wound healing. *Invest Ophthalmol Vis Sci.* 2015;56:3673–3683.
7. Cao Q, Xu W, Chen W, et al. MicroRNA-184 negatively regulates corneal epithelial wound healing via targeting CDC25A, CARM1, and LASP1. *Eye Vis (Lond).* 2020;7:35.
8. Stillman B. Histone modifications: insights into their influence on gene expression. *Cell.* 2018;175:6–9.
9. Kimura H. Histone modifications for human epigenome analysis. *J Hum Genet.* 2013;58:439–445.
10. Harada T, Hideshima T, Anderson KC. Histone deacetylase inhibitors in multiple myeloma: from bench to bedside. *Int J Hematol.* 2016;104:300–309.
11. Choudhary C, Kumar C, Gnad F, et al. Lysine acetylation targets protein complexes and co-regulates major cellular functions. *Science.* 2009;325:834–840.
12. Verdone L, Caserta M, Di Mauro E. Role of histone acetylation in the control of gene expression. *Biochem Cell Biol.* 2005;83:344–353.
13. Rahman S, Islam R. Mammalian Sirt1: insights on its biological functions. *Cell Commun Signal.* 2011;9:11.
14. Zhang X, Chen J, Sun L, Xu Y. SIRT1 deacetylates KLF4 to activate Claudin-5 transcription in ovarian cancer cells. *J Cell Biochem.* 2018;119:2418–2426.
15. Rahman I, Kinnula VL, Gorbunova V, et al. SIRT1 as a therapeutic target in inflammaging of the pulmonary disease. *Prev Med.* 2012;54(Suppl):S20–S28.
16. Granchi C, Minutolo F. Activators of Sirtuin-1 and their involvement in cardioprotection. *Curr Med Chem.* 2018; 25:4432–4456.
17. Hao C, Zhu PX, Yang X, et al. Overexpression of SIRT1 promotes metastasis through epithelial-mesenchymal transition in hepatocellular carcinoma. *BMC Cancer.* 2014;14:978.
18. Kunimoto R, Jimbow K, Tanimura A, et al. SIRT1 regulates lamellipodium extension and migration of melanoma cells. *J Invest Dermatol.* 2014;134:1693–1700.
19. Qiang L, Sample A, Liu H, et al. Epidermal SIRT1 regulates inflammation, cell migration, and wound healing. *Sci Rep.* 2017;7:14110.
20. Jaliffa C, Ameqrane I, Dansault A, et al. Sirt1 involvement in rd10 mouse retinal degeneration. *Invest Ophthalmol Vis Sci.* 2009;50:3562–3572.
21. Wang Y, Zhao X, Shi D, et al. Overexpression of SIRT1 promotes high glucose-attenuated corneal epithelial wound healing via p53 regulation of the IGFBP3/IGF-1R/AKT pathway. *Invest Ophthalmol Vis Sci.* 2013;54:3806–3814.
22. Hayashi Y, Call MK, Liu CY, et al. Monoallelic expression of Krt12 gene during corneal-type epithelium differentiation of limbal stem cells. *Invest Ophthalmol Vis Sci.* 2010;51:4562–4568.
23. Kalha S, Kuony A, Michon F. Corneal epithelial abrasion with ocular burr as a model for cornea wound healing. *J Vis Exp.* 2018;137:58071.
24. Ohata Y, Matsukawa S, Moriyama Y, et al. Sirtuin inhibitor Ex-527 causes neural tube defects, ventral edema formations, and gastrointestinal malformations in *Xenopus laevis* embryos. *Dev Growth Differ.* 2014;56:460–468.
25. Zhang X, Yuan Z, Zhang Y, et al. HDAC6 modulates cell motility by altering the acetylation level of cortactin. *Mol Cell.* 2007;27:197–213.
26. Singh BN, Zhang G, Hwa YL, et al. Nonhistone protein acetylation as cancer therapy targets. *Expert Rev Anticancer Ther.* 2010;10:935–954.
27. Shi L, Tu BP. Protein acetylation as a means to regulate protein function in tune with metabolic state. *Biochem Soc Trans.* 2014;42:1037–1042.
28. Latorre A, Moscardo A. Regulation of platelet function by acetylation/deacetylation mechanisms. *Curr Med Chem.* 2016;23:3966–3974.
29. Spallotta F, Cencioni C, Straino S, et al. Enhancement of lysine acetylation accelerates wound repair. *Commun Integr Biol.* 2013;6:e25466.
30. Spallotta F, Cencioni C, Straino S, et al. A nitric oxide-dependent cross-talk between class I and III histone deacetylases accelerates skin repair. *J Biol Chem.* 2013;288:11004–11012.
31. Hu X, Zhu S, Liu R, et al. Sirt6 deficiency impairs corneal epithelial wound healing. *Aging (Albany NY).* 2018;10:1932–1946.
32. Wang J, Lin A, Lu L. Effect of EGF-induced HDAC6 activation on corneal epithelial wound healing. *Invest Ophthalmol Vis Sci.* 2010;51:2943–2948.
33. Sebastian C, Satterstrom FK, Haigis MC, et al. From sirtuin biology to human diseases: an update. *J Biol Chem.* 2012;287:42444–42452.
34. Hu J, Kan T, Hu X. Sirt3 regulates mitophagy level to promote diabetic corneal epithelial wound healing. *Exp Eye Res.* 2019;181:223–231.
35. Lin Y, Li L, Liu J, et al. SIRT1 deletion impairs retinal endothelial cell migration through downregulation of

- VEGF-A/VEGFR-2 and MMP14. *Invest Ophthalmol Vis Sci.* 2018;59:5431–5440.
36. Hu Q, Wang G, Peng J, et al. Knockdown of SIRT1 suppresses bladder cancer cell proliferation and migration and induces cell cycle arrest and antioxidant response through FOXO3a-mediated pathways. *Biomed Res Int.* 2017;2017:3781904.
 37. Wilking MJ, Ahmad N. The role of SIRT1 in cancer: the saga continues. *Am J Pathol.* 2015;185:26–28.
 38. Schnoor M, Stradal TE, Rottner K. Cortactin: cell functions of a multifaceted actin-binding protein. *Trends Cell Biol.* 2018;28:79–98.
 39. Bryce NS, Clark ES, Leysath JL, et al. Cortactin promotes cell motility by enhancing lamellipodial persistence. *Curr Biol.* 2005;15:1276–1285.
 40. Motonishi S, Nangaku M, Wada T, et al. Sirtuin1 maintains actin cytoskeleton by deacetylation of cortactin in injured podocytes. *J Am Soc Nephrol.* 2015;26:1939–1959.
 41. Di Sante G, Wang L, Wang C, et al. Sirt1-deficient mice have hypogonadotropic hypogonadism due to defective GnRH neuronal migration. *Mol Endocrinol.* 2015;29:200–212.
 42. Schaks M, Giannone G, Rottner K. Actin dynamics in cell migration. *Essays Biochem.* 2019;63:483–495.